Available online at www.sciencedirect.com
SCIENCE DIRECT®

Journal of the European Ceramic Society 24 (2004) 2515–2526
www.elsevier.com/locate/jeurceramsoc

Flame assisted vapour deposition of cathode for solid oxide fuel cells. 1. Microstructure control from processing parameters

S. Charojrochkul*, K.L. Choy[1], B.C.H. Steele

Department of Materials, Imperial College of Science, Technology and Medicine, London SW7, UK

Received 28 February 2003; received in revised form 4 August 2003; accepted 14 August 2003

Abstract

The flame assisted vapour deposition (FAVD) technique has been used to deposit porous lanthanum strontium manganese oxide (LSM) to produce the cathode for a solid oxide fuel cell (SOFC). FAVD combines flame synthesis and vapour deposition methods where the liquid precursor undergoes a combustion process into a vapour phase, and then deposits as an oxide film on a substrate. The work has shown that the microstructures of deposited films may be dense or porous depending on processing parameters such as the deposition temperature, the concentration of the fuel and the distance between the spray nozzle and the substrate. A mechanism for the effects of these processing parameters interpreted as 'the combustion zone' has been proposed. This mechanism is used to explain the physical properties of films which were characterised using SEM and XRD. The FAVD technique is shown to be an efficient way in which SOFCs' cathode film can be fabricated with tailoring of the desired phases and microstructure.

Keywords: Cathodes; Flame assisted vapour deposition; Fuel oils; (La,Sr)MnO_3; SOFC

1. Introduction

Solid oxide fuel cells (SOFC) are being developed as efficient power generators. Difficulties involving the fabrication of the cell components, materials selection and high operating temperatures associated with SOFCs still have to be overcome before this technology becomes commercially viable. The present work involves the development of SOFC components fabrication, especially the cathode.

SOFC components can be fabricated via routes such as electrochemical vapour deposition (EVD) which is used commercially,[1] Chemical Vapour Deposition (CVD),[2] and Physical Vapour Deposition (PVD).[3] A novel method of Flame Assisted Vapour Deposition (FAVD) has been proposed to deposit a porous cathode film for SOFCs. This method has a similar principle to conventional CVD in which a film is deposited from the vapour phase.[4] Preliminary work showed the possibility of using this technique to deposit porous films of $La_{1-X}Sr_XMnO_3$ (LSM).[5–7] It is a cost effective method which yields a film of reasonable quality both in terms of microstructure and electrical properties.[6,7] The microstructure of LSM is required to be porous for the oxygen diffusion within the cathode to the three phase boundary between gas/cathode/electrolyte to take place.[8] The aim of the current research is to study the effect of processing parameters on the microstructure and phases present in deposited films. Consequently, some processing parameters such as the amount of fuel and the effect of droplet size (from the air pressure variation) have been modelled using the Computational Fluid Dynamic software package FLUENT. The results obtained from this model have been used to support the experimental results. The detail of the modelling work is described in a subsequent paper.[9]

2. Experimental procedures and setup

2.1. Preparation of a dense YSZ electrolyte substrate

An 8 mol% Y_2O_3 stabilised ZrO_2–YSZ was selected as the SOFC electrolyte. Commercial YSZ powder

* Corresponding author at present address: National Metal and Materials Technology Center, Thailand.
E-mail address: sumittrc@mtec.or.th (S. Charojrochkul).
[1] Presently at School of Mechanical, Materials, Manufacturing Engineering and Management, University of Nottingham, UK.

0955-2219/$ - see front matter © 2003 Elsevier Ltd. All rights reserved.
doi:10.1016/S0955-2219(03)00717-9

(supplied by Tosoh, Japan) was pressed into green body pellets of 10 mm in diameter by around 0.5–0.7 mm in thickness. The pellets were then sintered in air at 1500 °C for 2 h to produce densities greater than 98%.

2.2. Preparation of the precursor solution

Metal nitrate compounds of La [99.9% $La(NO_3)_3xH_2O$], Sr [99 + % $Sr(NO_3)$], and Mn (98% $Mn(NO_3)_26H_2O$] supplied by Aldrich Chemicals, were dissolved in deionised water to the desired ratio of La:Sr:Mn = 0.82:0.18:1 and 0.61:0.18:1. Ethanol was added to increase the inflammability of the solution. The ratio of ethanol to water was varied from 50:50 to 80:20 while the concentration of the precursor was varied from 0.01 to 0.1M.

2.3. Flame Assisted Vapour Deposition (FAVD) set up

A dense YSZ substrate was heated by means of a hot plate and a flame torch (such as a bunsen burner). The precursor solution as prepared previously was sprayed through an air atomiser across the flame to the substrate situated vertically below the spray nozzle. The atomised precursor was in the form of fine droplets, which are assumed to be in the form of an aerosol. These droplets then combusted when ignited by a flame source. The deposition temperature was monitored using a thermocouple placed next to the substrate. The heat of combustion provided thermal energy during the decomposition and vapourisation of these droplets, which underwent vapour phase reactions, resulting in an oxide film being deposited on a substrate. The full details of FAVD are described in previous literature.[4–6] The effects of processing parameters were investigated by varying only one parameter at a time while the others were kept constant. The full range of experimental conditions are given in Table 1.

3. Characterisation techniques

The adhesion of the as deposited films was evaluated qualitatively using a simple scratch test with an adhesive tape. The deposition was considered powdery when some particles remained on the adhesive tape. The microstructures of the films were examined using scanning electron microscope (SEM). Phases present in the films were identified by X-ray diffraction using Theta-2 Theta setup (Philips PW1710, with Cu target).

4. Results and discussion

4.1. Effect of ethanol/water ratio in the precursor solution

The ratios of ethanol/water in the precursor solution were varied as stated in Table 1. These variations produced changes in the deposition temperature and the characteristics of the as-deposited films. The high ethanol/water ratio resulted in a high deposition temperature while the low ethanol/water ratio gave low deposition temperature. At 770–810 °C, the deposition temperature of the 80/20 ratio produced film with powder agglomeration as shown in Fig. 1(a). However, the powder produced was very fine, ~1 micron in diameter and could be removed easily. A uniform porous film of large particles (10–20 microns size) was obtained at the 70/30 ratio (650–690 °C) as in Fig. 1(b). In Fig. 1(c), the film was nearly dense but with some large particles from the 60/40 ratio deposited at 470–520 °C. SEM micrographs on the right reveal the cross-section of the deposited film where the film thickness can be estimated.

The XRD spectra of the 70/30 ratio sample showed sharp crystalline peaks of $La_{0.8}Sr_{0.2}MnO_3$ (JCPDF 40-1100) designated as LSM while the spectra of the 60/40 ratio showed only a few peaks of LSM on broad haloes

Table 1
Standard parameters and variations used in FAVD for each examining effect

Parameters variation	Conc. of precursor (Molar)	Ratio of ethanol/water	Flow rate of precursor (ml/min)	Distance between spray nozzle and substrate (cm)	Pressure of compressed air (psi)
Effect of ethanol/water ratio[a]	0.05	80/20, 70/30, 60/40	12	12	22
Effect of flow rate[b]	0.05	80/20	5.5, 10, 17	12	22
Effect of conc. of precursor[a]	0.1, 0.075, 0.05, 0.025, 0.01	70/30	12	12	22
Effect of pressure of air atomizer[a]	0.05	70/30	12	12	17, 22, 26
Effect of distance between nozzle and substrate[b]	0.05	80/20	12	8, 12, 16	22

[a] The ratio of La:Sr:Mn was 0.82:0.18:1.

(indicating amorphous structures) as shown in Fig. 2. No peaks were observed for any films deposited at lower ratio than 60/40 and lower deposition temperature. The result implied non-crystalline deposition.

The shapes of the flame during deposition (combustion of precursor solution) was observed and are shown schematically in Fig. 3. Three different flame configurations were produced by changing the deposition parameters: these are designated as combustion zone A, B, and C. The area of zone A is the least while zone B includes zone A, and zone C includes both zones A and B. The shape of the combustion zone was later found to have a marked effect on the microstructure of the deposited film. The effect of the thermal environments was reported by Wiedmann et al.[4] and Viguie et al.[10]

At a high ethanol ratio (80/20), the range of deposition temperature was high since ethanol acted as a fuel for combustion resulting in a combustion zone of *Shape C* as seen in Fig. 3. By the time all the combusting species reached the substrate, the temperature was high, since the combustion process still continued. The difference of temperatures in the combustion and the sub-

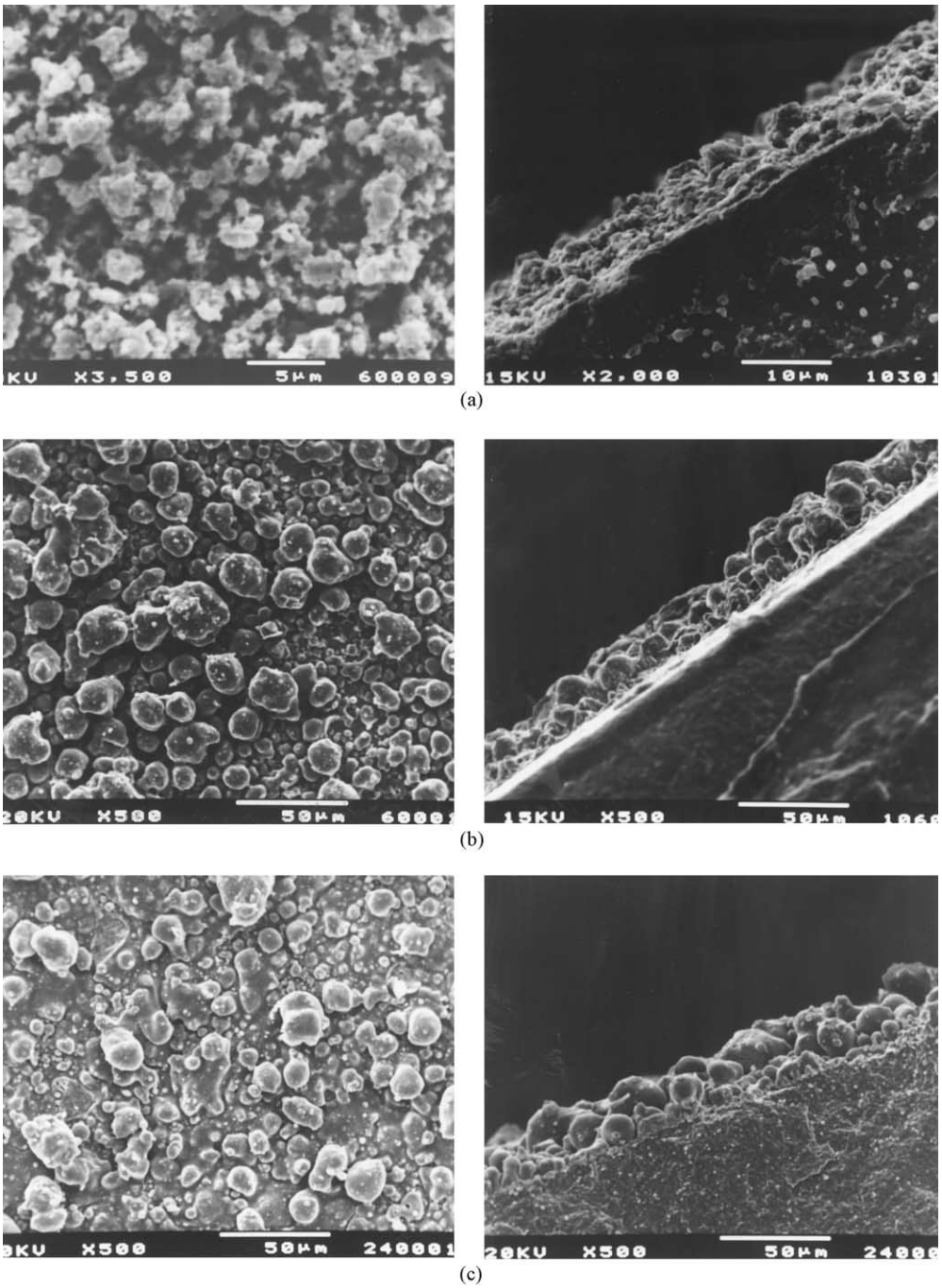

Fig. 1. Surface morphology of films deposited at various ratios of ethanol to water; (a) 80/20, (b) 70/30, and (c) 60/40.

strate was fairly low. Since the ratio of ethanol/water was high, the fuel was rich, most species combusted and reacted readily before reaching the substrate. As a result, the deposited particles were very fine as in Fig. 1(a) producing a powdery film. At high substrate temperature (700 °C), all the chemical reaction took place in the gas phase, in which the process was termed homogeneous gas phase nucleation.

When the ratio of ethanol/water was low enough (70/30) to yield the combustion zone of *Shape* B, the

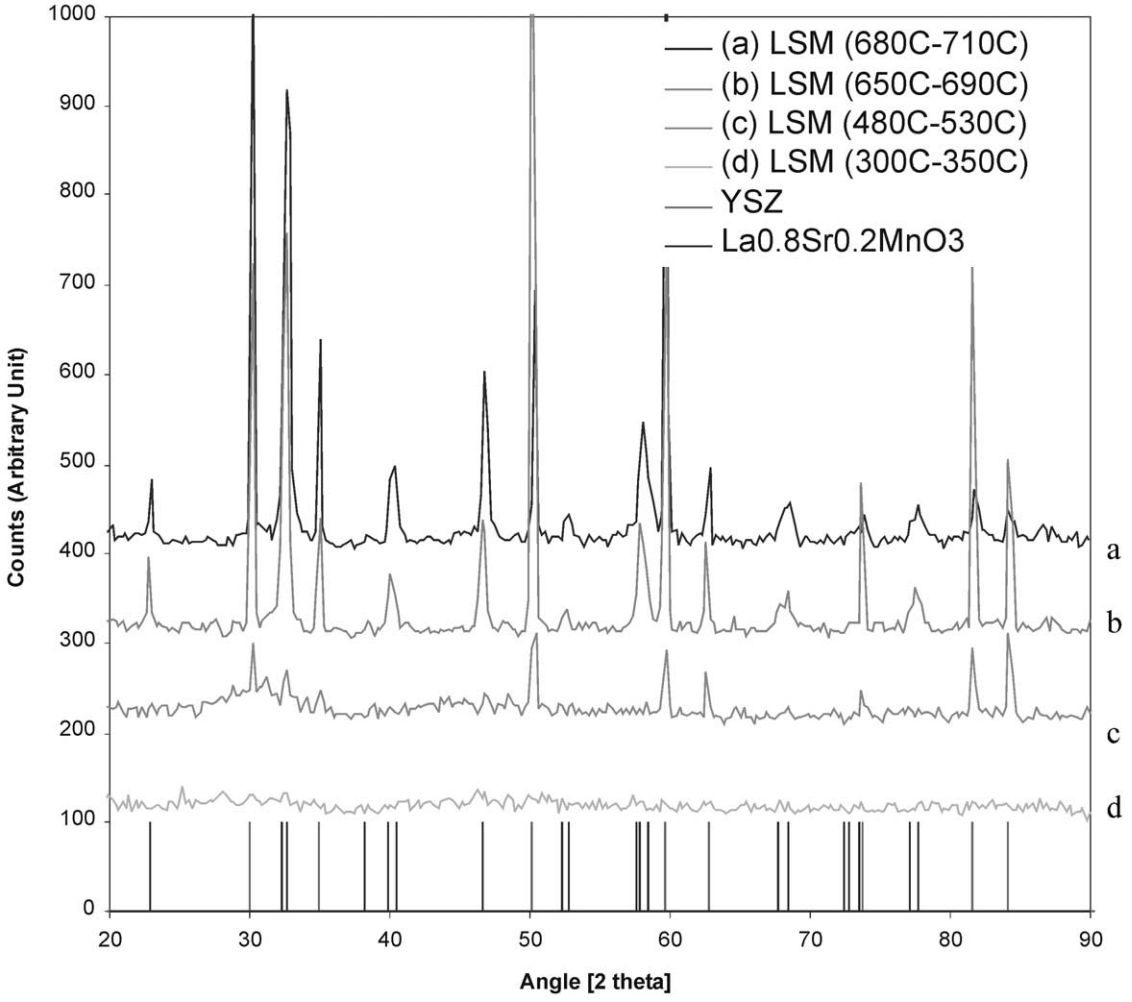

Fig. 2. XRD patterns of LSM films deposited at (a) 680–710 °C, (b) 650–690 °C, (c) 480–530 °C, and (d) 300–350 °C.

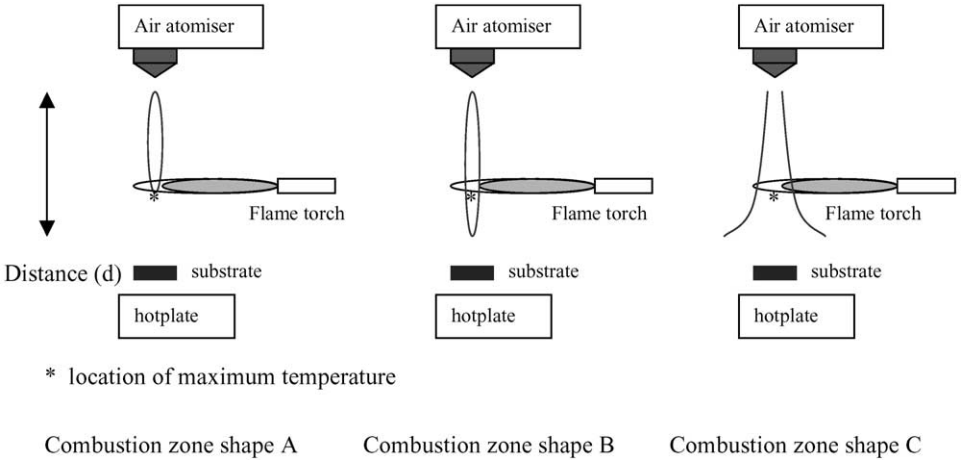

Fig. 3. A sketch of various combustion zones in the FAVD method.

deposition temperature was reduced. The heterogeneous nucleation reaction occured at the vicinity of the substrate resulting in a dense film as in Fig. 1(c). The maximum temperatures in the combustion zone of *Shape B* and *Shape C* were approximately the same, which was around 1000 °C. The maximum temperature at the tip of the flame torch was around 1200 °C. However, the heat convected/radiated to the substrate of combustion zone *Shape B* was lower than that of *Shape C* from the greater distance between the combustion and the substrate. In *Shape C*, the combustion was not complete within the combustion zone, therefore some aerosol droplets agglomerated and deposited as a porous film. During the deposition, particles grew and formed a densely packed film as in Fig. 1(b).

The combustion zone of *Shape A* only occured when the ratio of ethanol/water was very low (below 60/40) in that the fuel was not sufficient to combust all the droplets. The droplets then splashed onto the heated substrate. The solvent evaporated while leaving traces of dry precipitate, producing a flaky, amorphous film (Fig. 2(d)) as the decomposition of fuel and ions was not complete. The deposition temperature was very close to the temperature at the hot plate. The mechanisms are summarised in Fig. 4. The black open circle, grey open circle and black dot indicate an aerosol droplet, the reaction zone and the deposited particle respectively.

4.2. Effect of flow rate of the precursor solution

The flow rate of the precursor solution was varied from 5.5 ml/min to 17 ml/min whilst the deposition temperatures were controlled within the range of 700–800 °C. The microstructure of films deposited at the flow rate 5.5 ml/min, 10 ml/min, and 17 ml/min respectively are shown in Fig. 5.

At the low flow rate (5.5 ml/min), the combustion and decomposition reactions were completed in the gas phase, therefore the deposited film was powdery (the combustion zone of *Shape C*). At the high flow rate (17 ml/min), the reactions have not been completed by the time the droplets reached the substrate but continued to react at the vicinity of the substrate, resulting in a relatively dense film (the combustion zone of *Shape B*). Nevertheless, some cracks were present in the dense film probably due to thermal stresses on the thin dense film (around 4 microns thick). This dense film was not as resistant to cracking as a porous film. At the medium flow rate (10 ml/min), the film was a combination of particles and dense film resulting in a porous film.

The XRD patterns in Fig. 6 of various flow rate depositions showed the difference mainly for the substrate peaks. The film produced from the high flow rate (17 ml/min) deposition was much denser than the powdery film produced at a lower flow rate (5.5 ml/min).

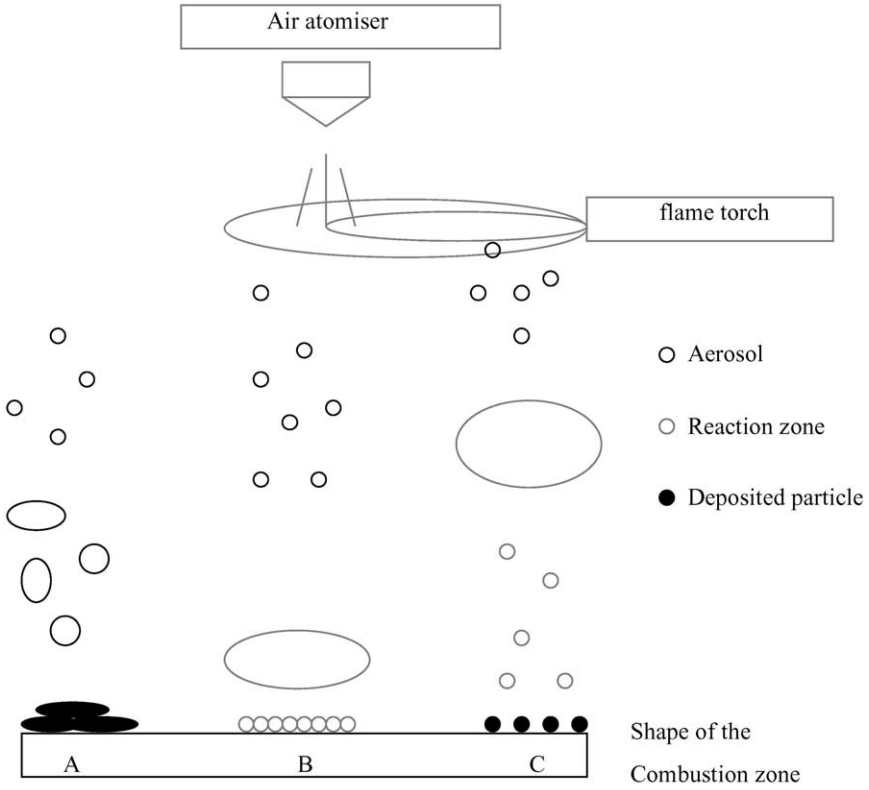

Fig. 4. A sketch of the relationship between the combustion zone and the deposition process.

The substrate peaks were more easily detected (referring to a thinner layer) and the powdery layer was more crystalline than the film deposited at the high flow rate. The LSM peaks were very similar in the shapes and degree of crystallinity.

4.3. Effect of concentration of the precursor solution

Fig. 6 shows the microstructures of the deposited films at various concentrations. The sizes of particles in the films varied with the concentration when they were deposited at the same ratio of ethanol/water. From the SEM micrographs, the size of particles was largest at high concentration (0.1 M) and smallest at low concentration (0.01 M). The degree of agglomeration also depended on the concentration of the precursor. More agglomeration was obtained at high precursor concentration, which also produced large particles as in Fig. 6(a). The porosity of the film was influenced by these parameters to form a large particle size with a high degree of agglomeration, associated with a high porosity fraction. The films showed less degree of agglomeration at reduced concentration when individual and finer particles became more distinctive. The film was the most powdery at the least concentration as seen in Fig. 6(e).

The effect of precursor concentration on microstructure can be described as the compaction of particles. When individual particles were close to each other from high concentration solution, they agglomerated. At low concentration, particles were far from each other and deposited as individual particles.

A similar influence has also been observed by Zhang and Messing[11] in using a spray pyrolysis technique to produce zirconia particles, the size of particle formed depended on the concentration of the solution. The size of particles was smaller when the concentration of solution was reduced.

4.4. Effect of the air atomiser pressure

The range of pressure variation of between 17 and 30 psi was restricted by the experimental setup. Fig. 7 shows large variations in the microstructure with the changes in compressed air pressures in the atomiser. The deposition temperature was controlled by the combination of all the parameters. At low pressure (17 psi), the film was powdery with fine particle sizes, smaller than 2 microns when the deposition temperature was at 720–770 °C. Particles in the film became connected at higher pressure as in Fig. 7(b) at 22 psi and the deposi-

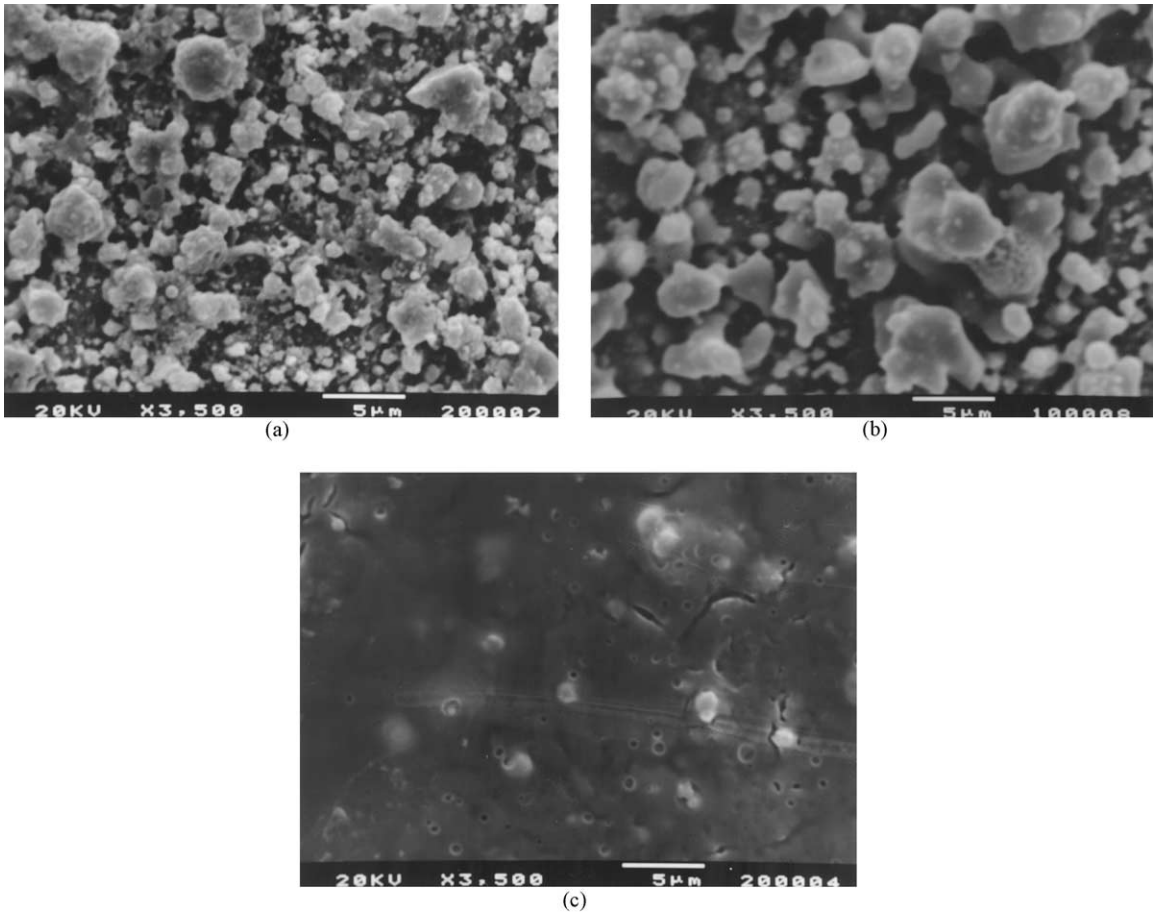

Fig. 5. Surface morphology of films deposited at (a) 5.5 ml/min, (b) 10 ml/min, and (c) 17 ml/min.

tion temperature was reduced to 680–730 °C. When the air pressure was increased further, the film was more densely packed with larger particle sizes of up to 20 microns in Fig. 7(c). However, some cracks were observed due to high air pressure producing high flow rate of cold air to chill the deposited surface. The deposition temperature was lowered to 450–500 °C.

The XRD patterns in Fig. 8 show that the crystallinity of deposited films was seen to be similar. The substrate peaks from the deposition at 17 psi were more obvious, due to the film being a thin powdery layer. The LSM film deposited at 26 psi was not electrically conducting and the associated XRD indicated an amorphous phase. After annealing at 900 °C for 2 h, this film became crystalline and electrically conducting. The film deposited at 17 psi showed traces of $La_2Zr_2O_7$ phase. This reaction product is undesirable for the SOFC cathode. However, it is commonly detected for low Sr dopant

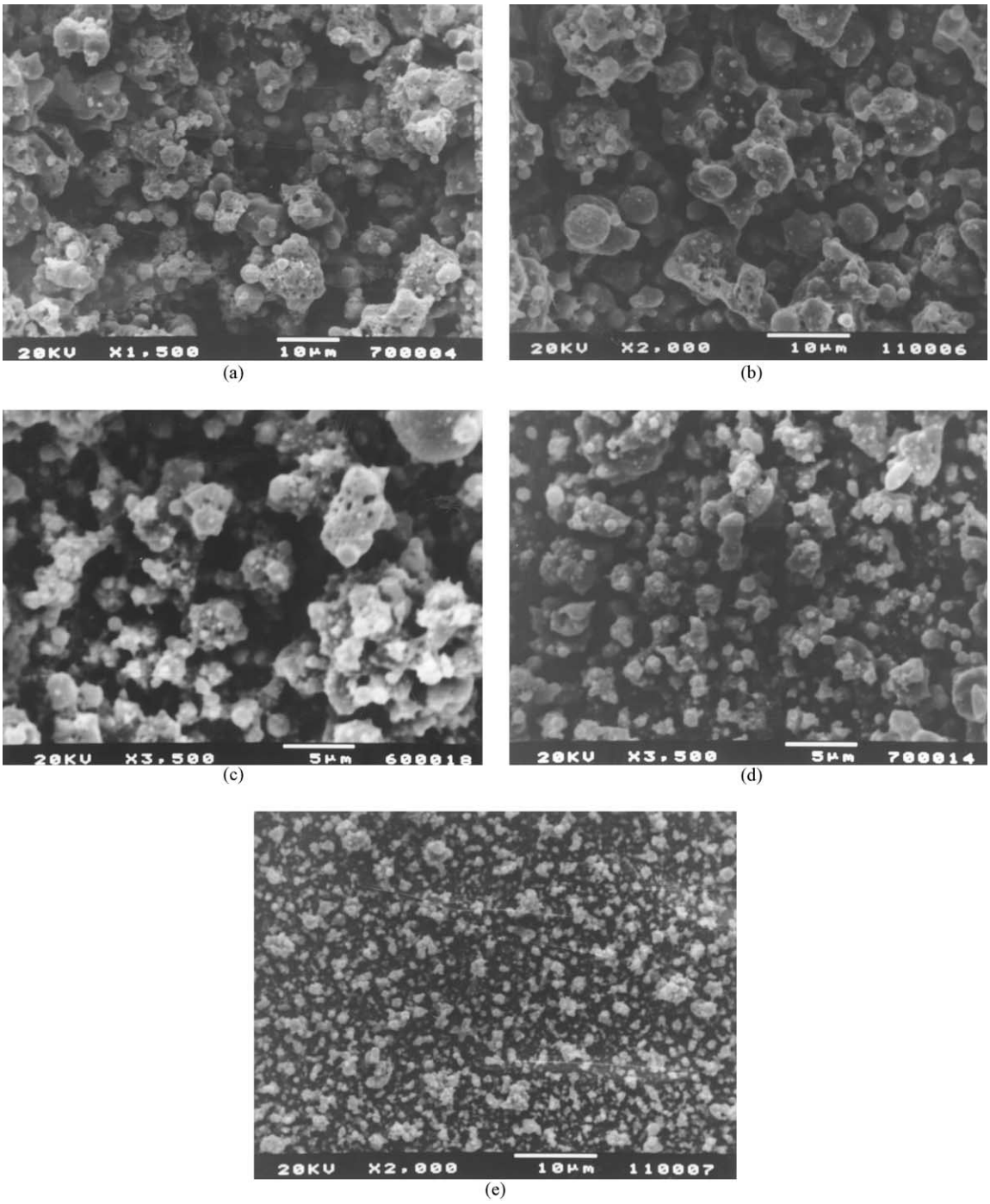

Fig. 6. Surface morphology of $La_{0.82}Sr_{0.18}MnO_3$ deposited from ethanol/water ratio of 70/30 of (a) 0.1 M, (b) 0.075 M, (c) 0.05 M, (d) 0.025 M, and (e) 0.01 M.

concentration as manganese diffuses to YSZ and the remaining lanthanum reacts with YSZ. $La_2Zr_2O_7$ has poor electrical conductivity and the coefficient of thermal expansion is not compatible with that of YSZ.[12–14] This acts as an insulating layer and creates thermal stresses at the interface.[15]

The total mass flow was the sum of the precursor solution and the compressed air. When the compressed air pressure was reduced, the amount of compressed air in the flow decreased, but it raised the ratio of the precursor solution in the total mass flow. As a result, the deposition temperature was increased in the higher fuel for combustion (higher ratio of solution to air). The compressed air was at room temperature therefore, it was acting as a stream of cool air and hence lowered the deposition temperature dramatically when the compressed air pressure was increased. The effect of deposition temperatures on the microstructures of the films was similar to the effect of ethanol/water ratio in the precursor solution. Fig. 9 shows a sketch of deposition processes at various compressed air pressures. At low air pressure, the deposition process followed the flame pattern of combustion zone of *Shape C* which yielded powdery film. At high air pressure, the flame pattern of this deposition process was similar to the combination of combustion zone of *Shapes B* and *C* producing a deposit of agglomerated particles.

4.5. Effect of the distance between the air atomiser and the substrate

The distance between the air atomiser and the substrate (d) was varied within the range of 8–16 cm as the shorter or longer distances had proven to be impractical. The surface morphology of the films produced at different distances are shown in Fig. 10. At a distance of 8 cm, the deposition temperature fluctuated tremendously from 500 to 830 °C resulting in a smooth film with fine pores and a lot of large cracks [Fig. 10 (a)]. The adhesion of the coating to the substrate was also very poor. At 12 cm, the film was uniformly porous with some agglomeration as in Fig. 10(b) and the normal range of deposition temperature (700–800 °C) was observed. At the longest distance of 16 cm, the deposition temperature varied widely again from 560 to 730 °C. The film produced was very powdery as in Fig. 10(c).

The $La_{0.8}Sr_{0.2}MnO_3$–LSM (JCPDF 40-110) phase was detected in all deposited films however the traces of

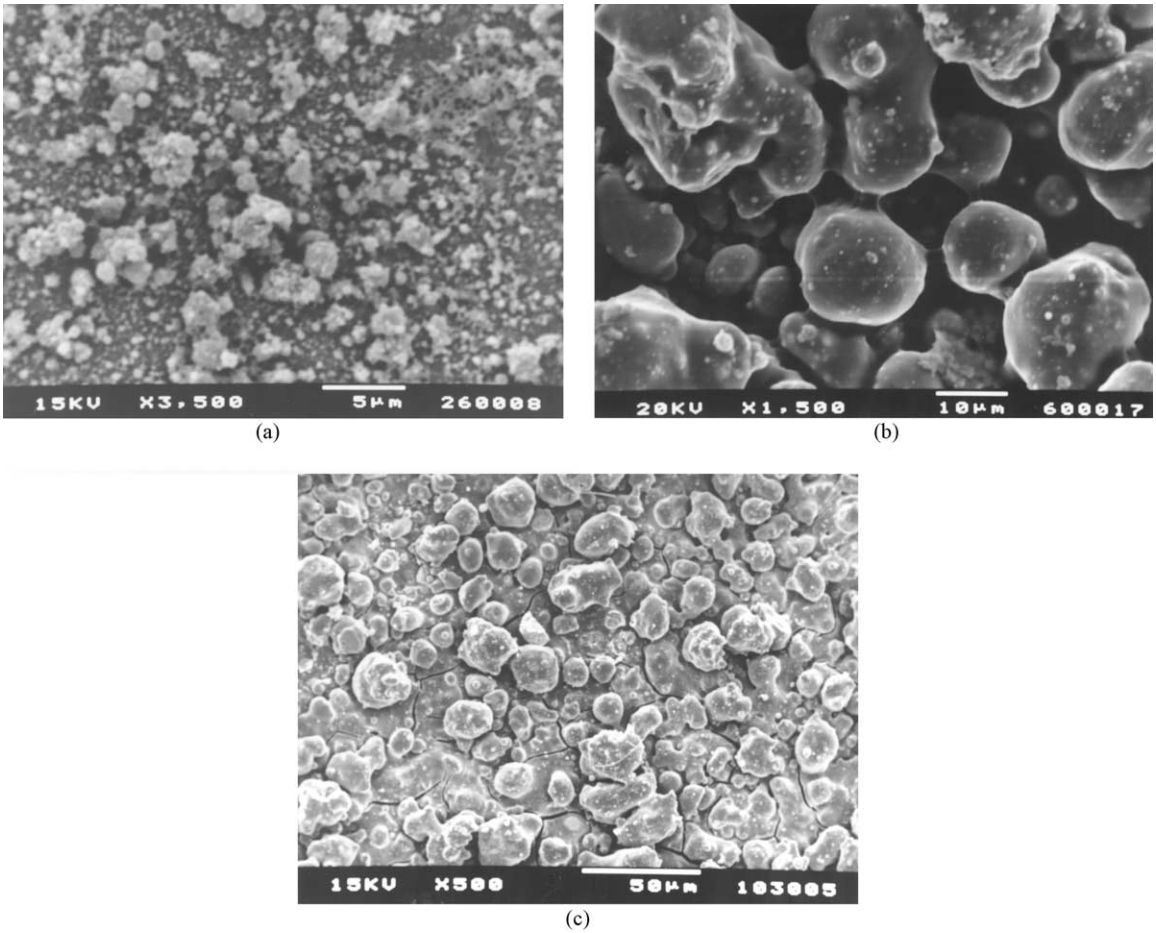

Fig. 7. Surface morphology of $La_{0.82}Sr_{0.18}MnO_3$ films deposited at (a) 17 psi, (b) 22 psi, and (c) 26 psi.

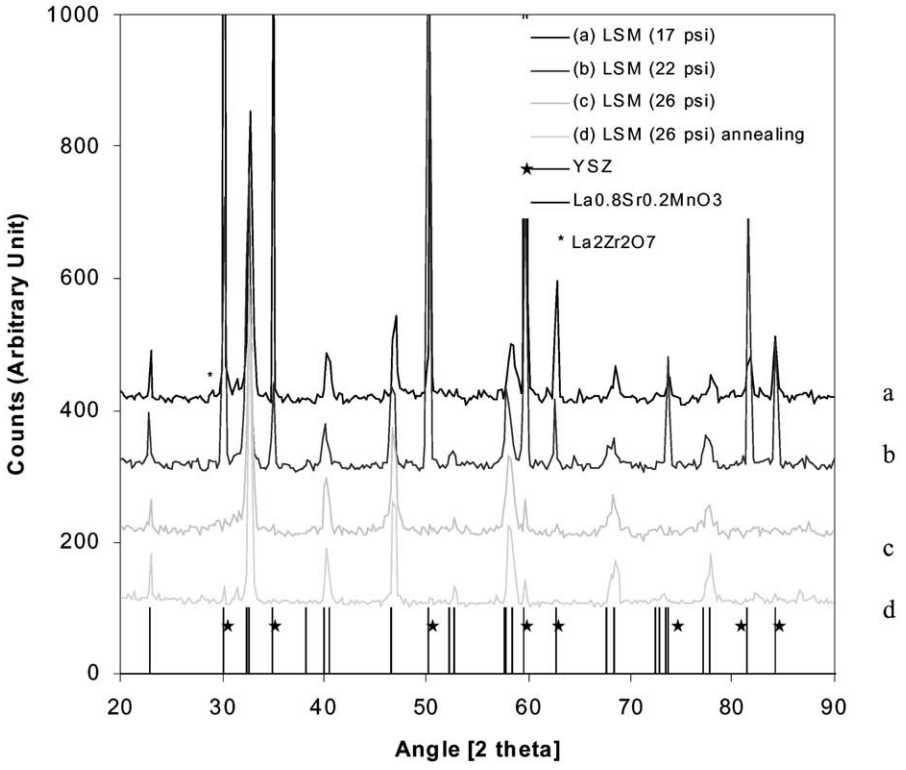

Fig. 8. XRD patterns of LSM films deposited at (a) 17 psi, (b) 22 psi, (c) 26 psi, and (d) 26 psi after annealing.

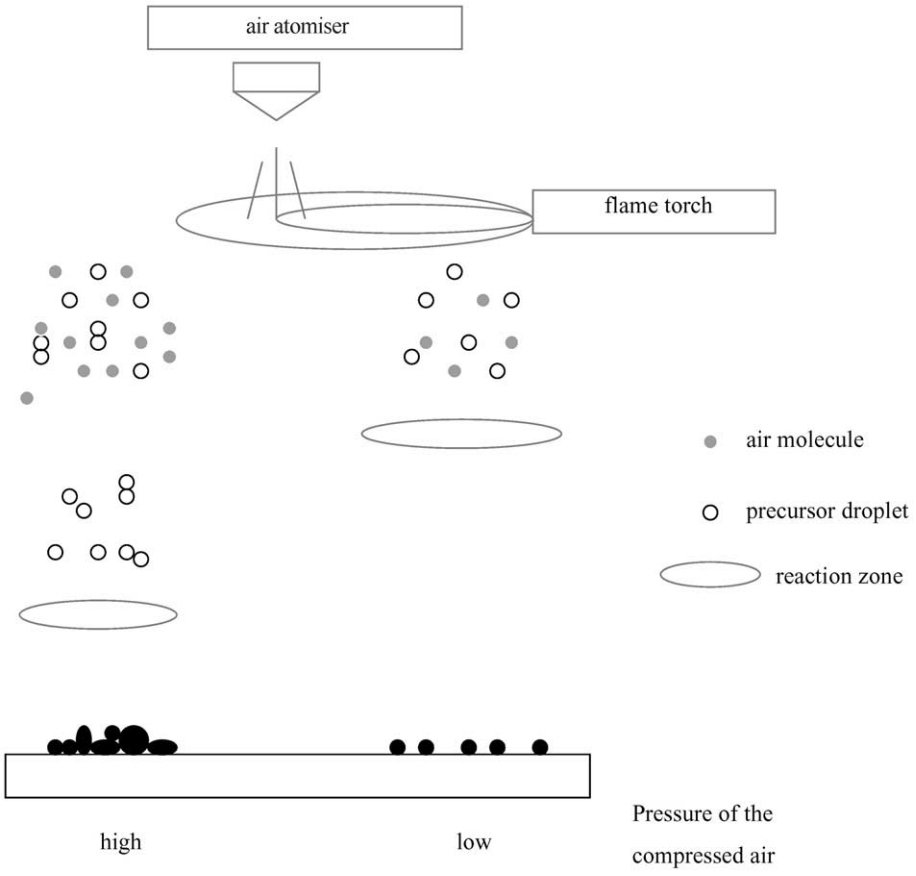

Fig. 9. A sketch of deposition processes at various compressed air pressures.

impurities found were different. The XRD pattern of the film from distance 8 cm indicated an amorphous phase and LSM phase of low degree of crystallinity, while the pattern of longer distances showed more crystalline films. Peaks representing $La_2Zr_2O_7$ phase were detected in the pattern for the distance 16 cm film. These two patterns are displayed in Fig. 11. In conclusion, both distances are not suitable for a SOFC

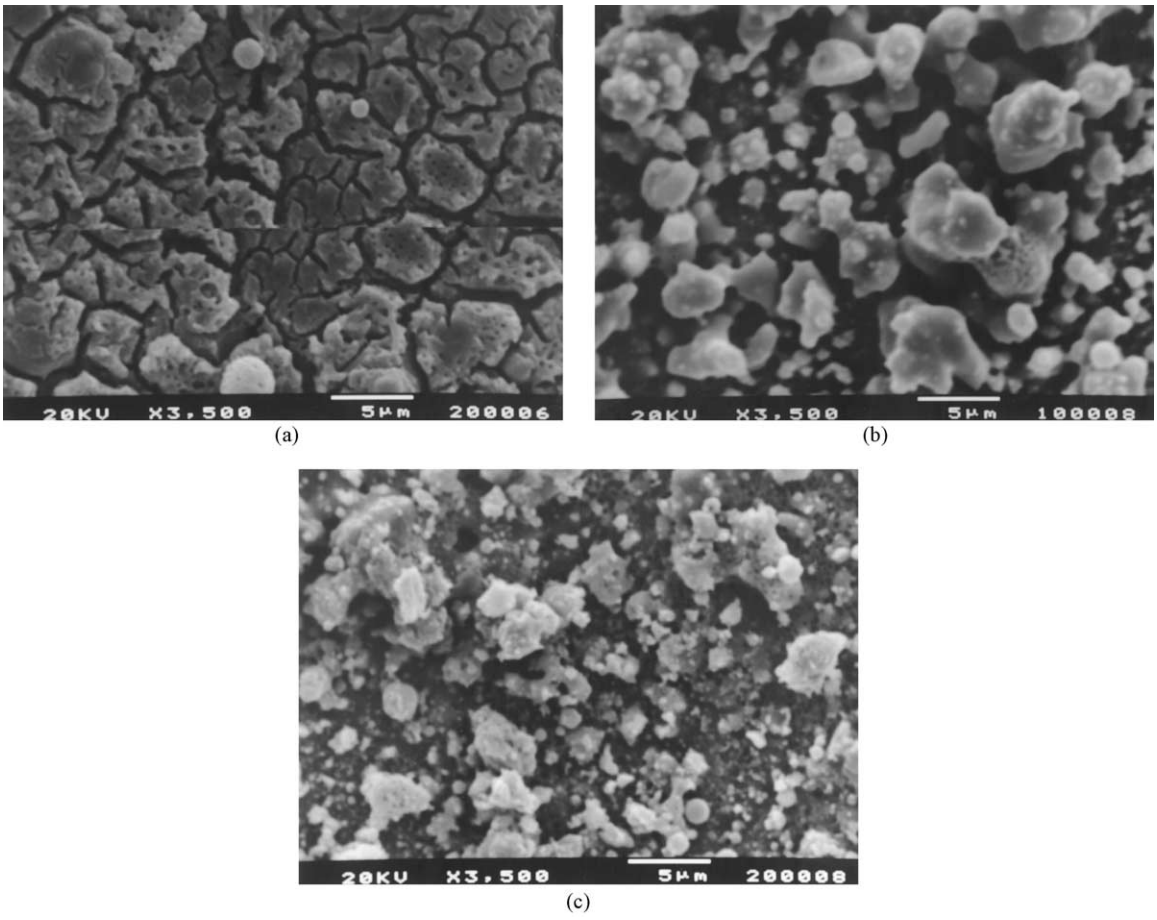

Fig. 10. Surface morphology of $La_{0.61}Sr_{0.18}MnO_3$ films deposited at distance (a) 8 cm, (b) 12 cm, and (c) 16 cm between the spray nozzle and the substrate.

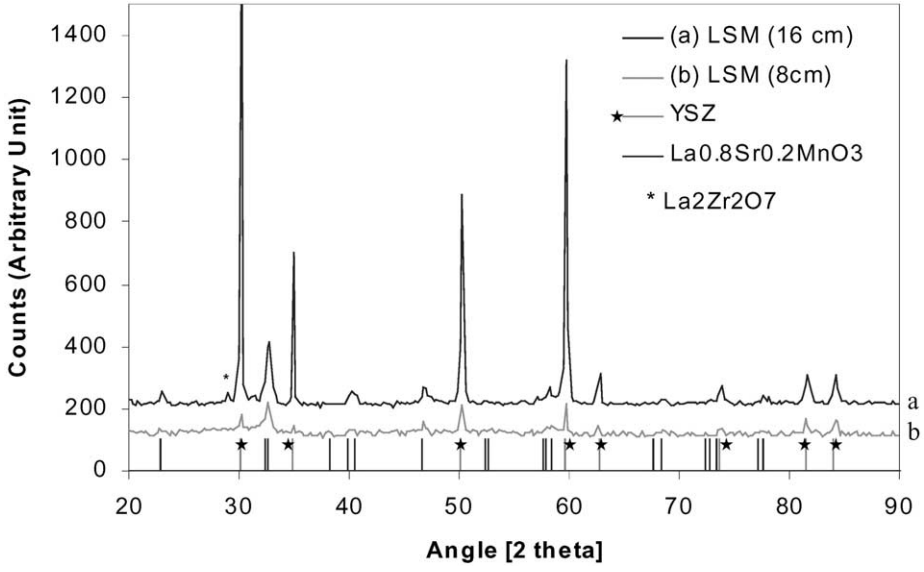

Fig. 11. XRD patterns of films deposited at distance (a) 16 cm and (b) 8 cm between the spray nozzle and the substrate.

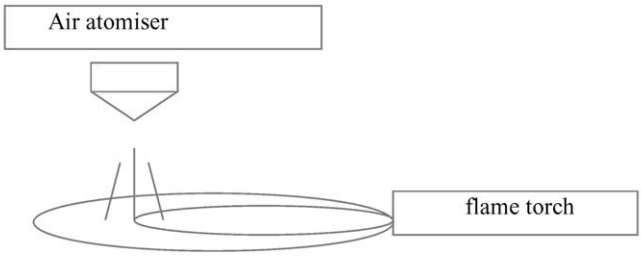

8 cm		Precursor droplets	A
12 cm		Reaction zone	B
16 cm		Deposited particles	C
Distance *d*		Characteristics of deposit	Shape of the combustion zone

Fig. 12. A sketch of the deposition process at various distances in the combustion zone.

cathode application. The most applicable distance is at 12 cm which is in between with combination of crystallinity and without the second phase.

At the distance 8 cm, the substrate was very close to the combustion zone and as a result, the droplets were deposited as a dense film. This was because the combustion and decomposition reactions took place at or near the surface of the substrate. Nevertheless, when the distance was too low, cracks were obvious from thermal shock effects due to pulses from the precursor pump. When d was at 16 cm, the combustion process was complete prior to reaching the substrate. The dominant reaction was the homogenous gas phase nucleation in which all the particles were produced prior to reaching the substrate. Moreover, by the time the droplets reached the substrate, the momentum was reduced and the particles did not pack, resulting in a powdery surface. The relationship between d and the deposition process in the combustion zone is shown in Fig. 12.

5. Conclusions

In FAVD, films deposited at high temperature (700–800 °C) were more powdery and crystalline than those from lower temperature deposition. The dominant reaction at high temperature deposition was governed by the gas phase nucleation. The temperature can be raised either by increasing the amount of ethanol in the precursor solution or increasing the mass fraction of ethanol, or adjusting the position of the flame torch. At lower temperatures where heterogeneous reactions were dominant, the decomposition and combustion reactions occured in the gas phase at or near the heated substrate, which resulted in dense film.

A desired porous LSM cathode film could be deposited using the following condition: concentration of 0.05 M of the precursor, the ratio of ethanol/water at 75/25, 12 ml/min flow rate, 12 cm distance between the spray nozzle and the substrate and the pressure of the compressed air fixed at 22 psi. The required phases and amount of porosity are necessary for the reduction of oxygen at the cathode which leads to a better performance of SOFCs.

Acknowledgements

S. Charojrochkul wishes to express her gratitude to the Government of Thailand for the financial support through her PhD scholarship. Thanks to Mr. R. Sweeney for the XRD analysis. Professor D.R. Fray and Professor J.A. Kilner are greatly acknowledged for their useful comments. The author would like to thank all the comments and suggestions from Dr. C. Chanyavanich, Dr. J. Pearce, Dr. A. Manonukul and Assoc. Professor S. Assabumrungrat.

References

1. Bratton, R.J., Reichner, P. and Montgomery, L.W., 1986 Fuel Cell Seminar Abstracts, October 26–29, 1986, Tucson, AZ, 80.
2. Kim, Y. B., Yoon, S. G. and Kim, H. G. J., *Electrochem. Soc.*, 1992, **139**, 2559.
3. Thiele, E. S., Wang, L. S., Wang, T. O. and Barnett, S. A. J., *Vac. Sci. Technol.*, 1991, **49**, 3054.
4. Wiedmann, I., Choy, K. L. and Derby, B., Novel synthesis and processing of ceramics. In *British Ceramic Proceedings No. 53*, ed. F. R. Sale. The Institute of Materials, London, 1994, pp. 133.
5. Choy, K. L., Charojrochkul, S. and Steele, B. C. H., Fabrication of cathode for solid oxide fuel cells using flame assisted vapour deposition technique. *Solid State Ionics*, 1997, **96**, 49–54.
6. Charojrochkul, S., Choy, K. L. and Steele, B. C. H., Cathode/electrolyte systems for solid oxide fuel cells fabricated using flame assisted vapour deposition technique. *Solid State Ionics*, 1999, **121**, 107–113.
7. Charojrochkul, S., Evaluation of oxide cathodes fabricated via flame assisted vapour deposition technique. PhD thesis, Imperial College of Science, Technology and Medicine, University of London, London, 1998.
8. Steele, B. C. H., Materials for fuel cells. In *Encyclopedia of Advanced Materials, No. 18616RB007*, ed. D. Bloor, R. J. Brook, M. C. Flemings and S. Mahajan. Pergamon Press, London, 1994.
9. Charojrochkul, S., Lothian, R.M., Choy, K.L. and Steele, B.C.H., Flame assisted vapour deposition of cathode for solid oxide fuel cells: Part 2 Modelling of processing parameters DOI:10.1016/j.eurceramsoc.2003.08.008.
10. Viguié, J. C. and Spitz, J., *J. Electrochem. Soc.*, 1975, **122**, 585–588.
11. Messing, G. L., Zhang, S. C. and Jayanthi, G. V., *J. Am. Ceram. Soc.*, 1993, **76**, 2707–2726.
12. Labrincha, J. A., Frade, J. R. and Marques, F. M. B.. In *Proceedings of the 2nd International Symposium on SOFCs, July 2–5, 1991, Athens, Greece*, ed. F. Grosz, P. Zegers, S. C. Singhal and O. Yamamoto. Commission of the European Communities, Luxembourg, 1991, pp. 689.
13. Labrincha, J. A., Frade, J. R. and Marques, F. M. B., *J. Mater. Sci.*, 1993, **28**, 3809.
14. Mori, M., Itoh, H., Mori, N., Abe, T., Yamamoto, O., Takeda, Y. and Imanishi, N.. In *Science and Technology of Zirconia V*, ed. S. P. S. Badwal, M. J. Bannister and R. H. J. Hennink. Technomic Publishing Company, Lancaster, 1993, pp. 776.
15. Minh, N. Q. and Takahashi, T., *Science and Technology of Ceramic Fuel Cells*. Elsevier Science BV, Amsterdam, 1995.